

Received: 5 September 2011 – Accepted: 27 November 2011 – Published: 19 December 2011

Correspondence to: J. Kim (jkim2@yonsei.ac.kr)

Published by Copernicus Publications on behalf of the European Geosciences Union.

33326

ACPD

11, 33325–33355, 2011

Aerosol optical depth retrieval from MODIS spectral reflectance

J. Lee et al.

Title Page

Abstract

Introduction

Conclusions

References

Tables

Figures

⏪

⏩

◀

▶

Back

Close

Full Screen / Esc

Printer-friendly Version

Interactive Discussion



Abstract

New over-ocean aerosol models are developed by integrating extensive AERONET inversion data and a database of the optical properties of tri-axial ellipsoidal dust particles. These models allow more accurate retrieval of aerosol optical depth (AOD) from the Moderate Resolution Imaging Spectroradiometer (MODIS) for high AOD cases. Spectral AOD, single scattering albedo (SSA), and phase function, which are used to calculate a lookup table (LUT), are archived by combining inversion data from Aerosol Robotic Network (AERONET) Sun/sky radiometers and single-scattering properties from the tri-axial ellipsoidal dust database. The aerosol models are categorized from the AERONET data using the fine-mode fraction (FMF) at 550 nm and the SSA at 440 nm to resolve a variety of aerosol types throughout the globe. For each aerosol model, the changes in aerosol optical properties (AOP) are included as functions of AOD. Comparisons of AODs between AERONET and MODIS for the period from 2003 to 2010 show that the new aerosol models improve correlation compared to the MODIS Collection 5 products with a Pearson coefficient of 0.93 and a regression slope of 0.99 compared to 0.92 and 0.85, respectively, for the MODIS operational algorithm. Moreover, use of the new algorithms increases the percentage of data within an expected error of $\pm(0.03 + 0.05 \times \text{AOD})$ from 62 to 64 % overall and from 39 to 51 % for high AOD cases ($\text{AOD} > 0.3$). Errors in the retrieved AOD are characterized further with respect to the Ångström exponent (AE), scattering angle (Θ), and air mass factor (AMF). Overall, the new aerosol models reduce systematic errors in AOD retrieval compared with the Collection 5 data due to realistic AOP assumptions. In particular, the scattering angle dependence of the retrieved AOD for dust cases is significantly mitigated due to improved treatment of the nonsphericity of dust particles by the new algorithm.

Aerosol optical depth retrieval from MODIS spectral reflectance

J. Lee et al.

Title Page

Abstract

Introduction

Conclusions

References

Tables

Figures

⏪

⏩

◀

▶

Back

Close

Full Screen / Esc

Printer-friendly Version

Interactive Discussion



1 Introduction

Aerosols exert a significant impact on climate change and air quality. These small airborne particles regulate the radiation budget through their direct and indirect effects (IPCC, 2007), or more specifically, by scattering and absorbing radiation and by modifying the microphysics of clouds. Aerosols are known to affect human health by causing and worsening respiratory illnesses (Pope and Dockery, 2006). Because the spatio-temporal distribution of aerosols is highly variable, satellite observations have been utilized extensively to quantify aerosol optical properties (AOP) over wide areas with fine spatio-temporal resolution.

Traditional 5-channel meteorological imagers, including single visible-band aboard geostationary satellites, are used to monitor aerosol optical depth (AOD) continuously, but have limited ability to retrieve other parameters (e.g., Knapp et al., 2002; Wang et al., 2003; Kim et al., 2008). In contrast, multi-spectral instruments onboard low Earth orbit (LEO) satellites, such as the Advanced Very High Resolution Radiometer (AVHRR), Sea-viewing Wide Field-of-view Sensor (SeaWiFS), and Moderate Resolution Imaging Spectroradiometer (MODIS), can retrieve aerosol size information and absorptivity (e.g., Higurashi and Nakajima, 1999; Mishchenko et al., 1999; Higurashi and Nakajima, 2002; Hsu et al., 2004; Remer et al., 2005; Hsu et al., 2006; Kim et al., 2007; Levy et al., 2007b). Recently, the Geostationary Ocean Color Imager (GOCI), which observes spectral radiances centered at 412, 443, 490, 555, 660, 680, 745, and 865 nm from a geostationary orbit, was used for hourly monitoring of AOD and to retrieve the fine-mode fraction (FMF) and aerosol types over East Asia (Lee et al., 2010b).

With their wide spatial and spectral coverage, the observations made by the MODIS instruments aboard the Terra and Aqua satellites provide an unprecedented opportunity to infer AOP. MODIS has 36 spectral bands ranging from 0.41 to 15 μm with three different spatial resolutions (250 m, 500 m, 1 km) and a 2300 km-wide swath coverage. Since the launch of MODIS in 1999 for Terra and 2002 for Aqua, numerous efforts have

Aerosol optical depth retrieval from MODIS spectral reflectance

J. Lee et al.

Title Page

Abstract

Introduction

Conclusions

References

Tables

Figures



Back

Close

Full Screen / Esc

Printer-friendly Version

Interactive Discussion



been made to retrieve, evaluate, and improve the aerosol products obtained. Kaufman et al. (1997) and Tanré et al. (1997) proposed original operational algorithms for dark vegetated areas and oceans, respectively. Since then, the MODIS algorithms have been updated to improve the quality of retrieved data by modifying cloud-masking processes, aerosol models, and the surface reflectance database (Remer et al., 2005; Levy et al., 2007a,b). In addition, Hsu et al. (2006) proposed the so-called Deep-Blue algorithm, which is applicable to bright land surfaces including desert areas, to facilitate monitoring of dust aerosols over the source region. Consequently, the current MODIS operational algorithms provide the columnar aerosol amount (AOD) and size information (FMF, Ångström exponent (AE)) with full coverage of the Earth except for cloud- and snow-covered areas. The Deep-Blue algorithm can also retrieve the single-scattering albedo (SSA) of dust aerosols.

MODIS aerosol products have been validated extensively to evaluate data quality. Preliminary comparisons of AOD from Terra-MODIS with that observed from Aerosol Robotic Network (AERONET) Sun/sky radiometers (Holben et al., 1998) showed that the AOD at 660 nm over the ocean differed by only 2 % on average from AERONET observations, with negligible offset (Remer et al., 2002), while the AOD over land was underestimated by about 14 % except for coastal areas (Chu et al., 2002). However, the comparison results for land varied significantly with location, partly due to different surface conditions and aerosol sources. On the contrary, a recent validation by Remer et al. (2008) showed an almost perfect regression slope for the AOD at 550 nm over land as calculated by AERONET and MODIS, but significant underestimation of AOD over the ocean from Aqua-MODIS in particular. It should be noted that the land algorithm has been modified substantially to resolve better aerosol models and surface reflectance (Levy et al., 2007a,b), whereas no substantial update has been made to the original ocean algorithm (Remer et al., 2005, 2006). Therefore, it is likely that the significant improvement in the regression slope over land is partly due to improved aerosol models, because the slope depends largely on data in the high AOD regime where the aerosol signal dominates the surface signal.

Aerosol optical depth retrieval from MODIS spectral reflectance

J. Lee et al.

Title Page

Abstract

Introduction

Conclusions

References

Tables

Figures

◀

▶

◀

▶

Back

Close

Full Screen / Esc

Printer-friendly Version

Interactive Discussion



In this paper, new aerosol models are introduced by integrating AERONET inversion data (Dubovik and King, 2000; Dubovik et al., 2006) and single-scattering property data from a tri-axial ellipsoidal dust database (Meng et al., 2010). The AOPs of each aerosol model are then used to calculate a lookup table (LUT) for spectral reflectances from MODIS. By using the LUT, retrieval and validation of AOD are performed over the global ocean using Aqua-MODIS, which improves the underestimation of AOD reported by Remer et al. (2008). Finally, the validation results are compared with those from the current operational algorithm to characterize further the effects of the new aerosol models.

2 MODIS ocean algorithms

Remer et al. (2005, 2006) described the current MODIS Collection 5 operational over-ocean algorithm (C005 algorithm hereafter) in detail. The algorithm retrieves spectral AOD and FMF using spectral reflectances centered at 555, 650, 860, 1240, 1630, and 2120 nm by comparing the observed and pre-calculated reflectances. To this end, sophisticated forward modeling simulating the observed reflectance (i.e. LUT) needs to be performed in advance for various sun and satellite geometries. Because the top-of-atmosphere (TOA) reflectance consists of signals from both the surface and atmosphere, the algorithm specifies surface reflectance in terms of the Fresnel reflection accounting for sea-surface roughness with a wind speed of 6 m s^{-1} and zero water-leaving radiance except for 550 nm where a water-leaving radiance of 0.005 is assumed. The atmospheric contribution, aerosols in particular, is calculated using four fine-mode and five coarse-mode aerosols. Then, both AOD and FMF are retrieved simultaneously by minimizing the error between the observed and calculated reflectances for each of the 20 combinations from the fine- and coarse-mode aerosol models, with the fixed AOD retrieved from 860 nm.

A schematic flowchart of the C005 algorithm and a test-bed algorithm to evaluate the effects of the new aerosol models introduced in this paper is provided in Fig. 1.

Aerosol optical depth retrieval from MODIS spectral reflectance

J. Lee et al.

Title Page

Abstract

Introduction

Conclusions

References

Tables

Figures



Back

Close

Full Screen / Esc

Printer-friendly Version

Interactive Discussion



The test-bed algorithm is designed to use the same spectral reflectances as the C005 algorithm to constrain other effects that can arise from different pre-processing of the data. We used the “Mean_Reflectance_Ocean” product in the “MYD04” files, which provides cloud- and sediment-masked mean reflectance in 20×20 pixels of 500 m pixel-resolution data at seven wavelengths centered at 470, 555, 650, 860, 1240, 1630, and 2120 nm. The product is the same as that used in the C005 algorithm. The major difference between the two algorithms is the aerosol model, while minor changes are made to the inversion procedure. The test-bed algorithm first retrieves AOD at 550 nm for all wavelengths and aerosol models, and then selects the most appropriate aerosol model that minimizes the standard deviation of the retrieved AODs at different wavelengths. In addition, the inversion algorithm uses longer wavelengths only (650, 860, 1240, 1630, 2120 nm) where the absorption of the water-body is strong enough to minimize errors from the assumed surface reflectance for $\text{AOD} \leq 0.15$, whereas for $\text{AOD} > 0.15$, it uses all seven bands. The algorithm retrieves AOD, FMF, and SSA simultaneously because the aerosol models are categorized by these parameters. Dimensions of the LUT used in the test-bed algorithm are summarized in Table 1.

3 New aerosol models

Simulation of satellite-observed TOA reflectance using a radiative transfer model (RTM) requires aerosol characteristics such as spectral refractive indices, size distribution, and nonsphericity when resolving nonspherical particles. Otherwise, spectral AOD, SSA, and phase function, which are derived from the aforementioned aerosol properties, are required instead. Thus, long-term AERONET inversion data that provides AOP for the globe can be used to simulate the satellite signal for various aerosol types. It should be noted that AERONET observes ambient-columnar properties similar to those obtained from satellite observations, while in-situ measurements provide near-ground properties. Moreover, the AOP retrieved from AERONET represents the radiation field well in the wide scattering angle range because the inversion data are retrieved in such

Aerosol optical depth retrieval from MODIS spectral reflectance

J. Lee et al.

Title Page

Abstract

Introduction

Conclusions

References

Tables

Figures



Back

Close

Full Screen / Esc

Printer-friendly Version

Interactive Discussion



a way to match the calculated radiation field with the observed sky radiances from the combined principal/almucantar planes (Dubovik and King, 2000; Dubovik et al., 2006). The inversion data, however, provide AOP at four-wavelengths ranging from 440 nm to 1020 nm, requiring the tri-axial ellipsoidal dust database introduced in the work of Meng et al. (2010) to be utilized to expand the wavelength range up to 2120 nm for MODIS observations.

3.1 AERONET inversion data

The quality-assured, “Level 2 Inversion All Points” data are used to derive aerosol models over the ocean for the test-bed algorithm. To this end, AERONET stations are sorted first by distance from the ocean, calculated using geo-location information for each AERONET site and a high-resolution digital elevation model (DEM). The coastal stations are then selected based on the criterion of a distance of less than 7 km from the ocean. Figure 2 shows the 81 selected stations and the number of inversion data available to date. Although large portion of the data are from the US and Europe, where anthropogenic aerosols are dominant, the AERONET data in the downwind of North Africa are expected to provide AOPs of transported dust and biomass-burning aerosols. The data also cover dust aerosols transported from the Arabian Desert, both anthropogenic and dust aerosols over East Asia, and marine aerosols over the remote ocean. However, only one site is located in downwind of Southern Africa, which may lead to uncertainties in the AOP of biomass-burning aerosols from this area.

Aerosol models incorporated in satellite algorithms should account for the various aerosol types that exist and cause differences in the radiation field, so that the appropriate aerosol models can be selected from the observed radiation field. Therefore, classification of aerosol types using their size and absorptivity is the most reasonable method for remote sensing because these two parameters directly affect the radiation field (Dubovik et al., 2002; Levy et al., 2007a; Mielonen et al., 2009; Lee et al., 2010a). While MODIS operational algorithms adopt fine- and coarse-mode aerosols separately and then combine their signals during retrieval, the test-bed algorithm adopts

Aerosol optical depth retrieval from MODIS spectral reflectance

J. Lee et al.

Title Page

Abstract

Introduction

Conclusions

References

Tables

Figures



Back

Close

Full Screen / Esc

Printer-friendly Version

Interactive Discussion



independent mixture-type models by classifying aerosol types from AERONET explicitly with respect to the FMF at 550 nm and the SSA at 440 nm (Lee et al., 2010b).

Figure 3 shows the number of aerosol events with specific FMF and SSA values observed by AERONET throughout the globe and in coastal areas. As shown in Fig. 3a, aerosols from different locations have a wide range of FMF and SSA values, indicating the presence of various aerosol types from small to large particles and from absorbing to non-absorbing particles. For FMF less than 0.4 (coarse-mode dominance), the SSA generally ranges from 0.85 to 0.95, indicating absorption of blue-wavelengths by the coarse particle-dominated aerosols. Because Level 2 inversion data provides SSA for AOD (440 nm) > 0.4 , the coarse particle-dominated aerosols mainly represent dust events. Note that sea-salt, non-absorbing coarse-mode aerosol, generally occur at low AOD values. For fine particle-dominated aerosols (FMF > 0.6), the range of values for SSA is wider than that for coarse particle-dominated aerosols. The high SSA values correspond to non-absorbing anthropogenic aerosols, such as sulfate and nitrate, whereas the low SSA values imply the presence of black carbon (BC) (Hess et al., 1998; Wang and Martin, 2007). The major difference in AOP between global and coastal data is highlighted by the lack of data in the extremely low SSA regime. This can be explained by the high relative humidity (RH) in coastal areas, aging of BC during transport, and too few AERONET stations in downwind of biomass-burning aerosols that show low SSA. Both high RH and aging of BC are known to increase SSA (Wang and Martin, 2007).

Based on the representativeness of aerosol types classified using FMF and SSA (Lee et al., 2010a), aerosol models are created by quantized square-bins over the FMF and SSA domains. Binning intervals of 0.1 and 0.05 are used for FMF and SSA, respectively. Each aerosol model is then further categorized as a function of AOD by averaging AOP between fore- and aft-medians of each AOD nodal point represented in Table 1. When there are no data for a higher AOD bin, the AOP of the previous bin is used instead. Consequently, spectral AOD, SSA, and phase function are averaged over the three-dimensional domains of FMF, SSA, and AOD. Prior to the averaging, spectral

Aerosol optical depth retrieval from MODIS spectral reflectance

J. Lee et al.

Title Page

Abstract

Introduction

Conclusions

References

Tables

Figures

◀

▶

◀

▶

Back

Close

Full Screen / Esc

Printer-friendly Version

Interactive Discussion



AOD is normalized by itself at 550 nm and multiplied by each AOD nodal point. This method, however, has limited application to low AOD data, because SSA is retrieved only for AOD (440 nm) > 0.4. As an alternative, SSA is assumed to be 0.99 regardless of the wavelength by considering the sea-salt dominance in the low AOD regime over the ocean, while the other parameters (spectral AOD, phase function) are archived from AERONET inversion data. As a result, a total of 23 aerosol models are created, with the number of data points constrained to be greater than 10 for each aerosol model. The aerosol models cover FMF ranging from 0.2 to 1.0 for $0.85 < \text{SSA} < 0.95$ (16 types), and from 0.3 to 1.0 for $\text{SSA} > 0.95$ (7 types).

3.2 Tri-axial ellipsoidal dust database

The AERONET inversion data provide AOP for wavelengths ranging from 440 to 1020 nm, while the MODIS observations cover the wavelengths from 470 to 2120 nm. To expand the wavelength range of AERONET AOP, data from the tri-axial ellipsoidal dust database (Meng et al., 2010) are used in this study. The database contains single-scattering properties of individual tri-axial ellipsoidal particles including spheres and spheroids for various refractive indices, particle sizes, and aspect ratios. The single-scattering properties in this database are computed using the Lorentz-Mie code (Bohren and Huffman, 1983), T-matrix code (Mishchenko and Travis, 1998), Amsterdam discrete dipole approximation (DDA) code (Yurkin and Hoekstra, 2009), and improved geometric optics method (IGOM) code (Yang and Liou, 1996; Yang et al., 2007; Bi et al., 2009). Because the AERONET inversion algorithm utilizes a similar database to retrieve AOP (Dubovik et al., 2006), the dust database can generate consistent data when refractive indices, size distribution, and nonsphericity are given. Among the aforementioned parameters, only refractive indices are a function of wavelength, so we decided to use the size distribution and nonsphericity from AERONET, and the refractive indices from the current MODIS algorithm (Remer et al., 2005, 2006) to derive spectral AOD, SSA, and phase function for longer wavelengths. The refractive indices of “water soluble” and “water soluble with humidity” from the MODIS

Aerosol optical depth retrieval from MODIS spectral reflectance

J. Lee et al.

Title Page

Abstract

Introduction

Conclusions

References

Tables

Figures

◀

▶

◀

▶

Back

Close

Full Screen / Esc

Printer-friendly Version

Interactive Discussion



aerosol models are used for fine-mode ($0.85 < SSA < 0.95$ and $SSA > 0.95$, respectively), while the refractive indices of “dust-like type” and “wet sea salt type” are used for coarse-mode ($AOD > 0.1$ and $AOD = 0.1$, respectively). Although the refractive indices of the MODIS aerosol models are not completely consistent with those of the new aerosol models, use of the TOA reflectance at these wavelengths can contribute to better FMF retrieval because of better sensitivity in discriminating particle sizes compared to shorter wavelengths, thus improving AOD retrieval. With regard to nonsphericity, mean “% sphericity” in the AERONET data is used with the fixed spheroid mixture distribution as described in Dubovik et al. (2006). The dataset archived by combining the AERONET inversion data and tri-axial ellipsoidal dust database data covering the full MODIS wavelength range is finally used to calculate a LUT to retrieve AOP.

4 Results and evaluation

The effects of the new aerosol models on AOD retrieval are evaluated by comparing AODs between AERONET and MODIS retrieved using C005 and the test-bed algorithm. Eight years of spectral reflectance data (2003–2010) observed from Aqua-MODIS are collected and processed to retrieve AOD using the new aerosol models. The AOD data from the C005 algorithm are also processed to compare with the AERONET observations, thereby allowing validation results from both algorithms to be compared. In this study, the “Effective_Optical_Depth_Average_Ocean” data in the MYD04 files are used for the C005 algorithm. Overall statistical scores and systematic errors are compared to characterize various error sources.

4.1 Overall evaluation

Figure 4 shows a comparison of AODs from AERONET and MODIS over the global ocean from 2003 to 2010. For this comparison, collocation was made within ± 30 min in time and 25 km in space as proposed by Ichoku et al. (2002). A criterion for the

Aerosol optical depth retrieval from MODIS spectral reflectance

J. Lee et al.

Title Page

Abstract

Introduction

Conclusions

References

Tables

Figures



Back

Close

Full Screen / Esc

Printer-friendly Version

Interactive Discussion



number of data points, which requires at least 5 and 2 data points for MODIS and AERONET, respectively, was also applied. For comparison, we sampled MODIS pixels by calculating the actual distance between AERONET and the center of each MODIS pixel, while Ichoku et al. (2002) selected 5×5 MODIS pixels around an AERONET station as a center, regardless of the viewing angle. Because a high viewing angle results in an increase in ground-pixel size, the number of data points compared in this study is less than that in the original method. Only overlapping data retrieved by both algorithms were used for quantitative comparison. The test-bed algorithm tended to retrieve more data than the C005 algorithm due to the absence of quality-control procedure used in C005 algorithm.

The validation results show that the AOD data from the C005 algorithm are highly correlated with the observations, but tend to be underestimated on average, with a Pearson coefficient of 0.92 and a regression slope of 0.85. The negative bias of the slope is caused by overestimation in the low AOD regime ($AOD < 0.2$) and underestimation in the high AOD regime ($AOD > 0.2$). In particular, the slope is largely affected by data in the high AOD regime. Meanwhile, the new aerosol models improve the slope significantly (0.99) with a comparable correlation coefficient (0.93). From the statistics summarized in Table 2a and Table 2b, it is clear that the aerosol models improve almost all statistics analyzed in this study. Not only the slope but also the percentage of data within an expected error of $\pm(0.03 + 0.05 \times AOD)$ improved from 62 to 64 % overall and from 39 to 51 % for $AOD > 0.3$. These improvements are particularly noticeable for the high AOD regime where the aerosol signal dominates other contributions, such as Rayleigh scattering and surface reflectance. The major reason for the improvement in AOD is the consideration of absorbing fine-mode aerosols and changing AOP, size distribution in particular, as a function of AOD. Both factors are expected to increase AOD for a given TOA reflectance (Levy et al., 2007b; Wang and Martin, 2007; Jethva et al., 2010). Note that the current MODIS algorithm adopts four-different water-soluble aerosol models with fixed radii insensitive to AOD for fine-mode cluster.

Aerosol optical depth retrieval from MODIS spectral reflectance

J. Lee et al.

[Title Page](#)[Abstract](#)[Introduction](#)[Conclusions](#)[References](#)[Tables](#)[Figures](#)[◀](#)[▶](#)[◀](#)[▶](#)[Back](#)[Close](#)[Full Screen / Esc](#)[Printer-friendly Version](#)[Interactive Discussion](#)

4.2 Error characteristics

Errors in AOD can arise from various sources including incorrect assumptions about surface reflectance and aerosol type, status of sensor calibration, observation geometry, etc. In addition, specific observation environments can bias results. The new aerosol models developed in this study are expected to reduce errors due to aerosol type and observation geometry including scattering angle and air mass. Levy et al. (2010) evaluated C005 AOD data over land with regard to AE, cloud fraction, surface type characteristics, and observation geometry to characterize systematic error sources. Thus, the analyses presented here together with the work of Levy et al. (2010) represent a complete evaluation of the MODIS data retrieved over ocean and land.

Figure 5 shows the AE dependence of the retrieval errors for the C005 and the test-bed algorithms. The data were sorted in 20 and 10 equal-number-of-data bins for the overall data and $AOD > 0.3$, respectively. As shown in Fig. 5a, the C005 algorithm in general tends to overestimate coarse-dominated AOD ($AE < 0.8$) and underestimate fine-dominated AOD ($AE > 1.6$). Underestimation of the fine particle-dominated AOD seems to be related to the high AOD because the C005 algorithm systematically underestimates AOD for the high AOD regime, as illustrated in Fig. 4. However, the algorithm overestimates the observed AOD for $0.2 < AE < 0.4$ even though the data show high AOD compared to the fine particle-dominated case. The retrieval products are less stable (stability inferred by the length of one standard deviation interval) for fine particle-dominated AOD than coarse particle-dominated AOD, while stable retrieval for $0.75 < AE < 1.4$ is observed, partly due to the relatively low AOD. In the case of $AOD > 0.3$, while there was systematic underestimation, the algorithm showed a small mean bias (MB) for strong dust events ($AE < 0.4$, high AOD) with higher stability than in the fine particle-dominated case ($AE > 1.4$).

The AE dependence of MB for the test-bed algorithm is reduced overall compared with the C005 algorithm, but the test-bed algorithm still has a tendency to overestimate coarse particle-dominated AOD and to underestimate fine particle-dominated AOD.

Aerosol optical depth retrieval from MODIS spectral reflectance

J. Lee et al.

Title Page

Abstract

Introduction

Conclusions

References

Tables

Figures

◀

▶

◀

▶

Back

Close

Full Screen / Esc

Printer-friendly Version

Interactive Discussion



The AE dependence is reduced further for $AOD > 0.3$, but the AODs are distinctly overestimated for coarse particle-dominated case ($AE < 0.3$). However, the standard deviation of the retrieval errors is lower than that of the C005 algorithm for the coarse particle-dominated regime, while the standard deviation is similar between the two algorithms for the fine particle-dominated regime ($AE > 1.3$). Therefore, the new aerosol models significantly reduce systematic error (i.e. MB) compared with the C005 algorithm except for severe dust events ($AOD > 0.3$, $AE < 0.3$).

Figure 6 shows an additional comparison of retrieval errors with regard to aerosol type and scattering angle for $AOD > 0.3$. Note that neglecting the nonsphericity of dust particles results in underestimation of AOD in the back-scattering direction, while it causes overestimation in the side-scattering direction due to difference in scattering phase function. For a dust-dominated case ($AE < 0.8$), the data provided by the C005 algorithm are an imprint of the difference in phase functions between spherical and nonspherical particles, while the new aerosol models significantly reduce the scattering angle dependence. The new aerosol models, however, systematically overestimate AOD regardless of scattering angle. Consequently, the small MB of the C005 algorithm for coarse particle-dominated AOD represented in Fig. 5 can be explained by canceling of the positive and negative errors, while the test-bed algorithm systematically overestimates AOD. For anthropogenic aerosols ($AE > 1.2$), neither algorithm shows distinct feature related to differences in phase function, while the systematic underestimation of the C005 algorithm in the back-scattering direction in particular is greatly reduced when the test-bed algorithm is used.

Figure 7 shows the scattering angle dependence of the retrieval errors. For the C005 algorithm, MB decreases gradually with increasing scattering angle, due to systematic underestimation with increasing AOD. In contrast, the scattering angle or AOD dependence of MB is much lower in the test-bed algorithm because of improved AOD data. Only two distinct positive peaks are present for $140^\circ < \Theta < 165^\circ$ where both anthropogenic and dust aerosols show positive MBs in Fig. 6. For $AOD > 0.3$, the underestimation increases with increasing mean AOD for $\Theta > 140^\circ$ by the C005 algorithm, but

Aerosol optical depth retrieval from MODIS spectral reflectance

J. Lee et al.

[Title Page](#)[Abstract](#)[Introduction](#)[Conclusions](#)[References](#)[Tables](#)[Figures](#)[⏪](#)[⏩](#)[◀](#)[▶](#)[Back](#)[Close](#)[Full Screen / Esc](#)[Printer-friendly Version](#)[Interactive Discussion](#)

the correlation between mean AOD and MB decreases with a higher standard deviation for the side-scattering direction where dust aerosols cause a positive error. For the test-bed algorithm, the MB shows positive values for $\Theta > 140^\circ$, and a negative bias for $\Theta < 140^\circ$, partly due to the combined effects of systematic overestimation of coarse particle-dominated AOD regardless of scattering angle and underestimation of fine particle-dominated AOD for $\Theta < 140^\circ$.

The sensitivity of TOA reflectance to AOD increases with air mass because of increasing optical path. Thus, the air mass factor (AMF), which is defined by $m_{\text{Sun}} \times m_{\text{satellite}}$ where $m = \sec(\theta)$ can affect retrieval accuracy. Figure 8 shows the AMF dependence of the retrieval errors. We expected that the retrieval errors would decrease with AMF because of increased sensitivity. However, the pattern that we observed was more complicated, because the retrieval errors are functions of AOD, Θ , and aerosol type (i.e. AE). For both algorithms, retrieval stability increases (decreasing standard deviation) with AMF partly because of increasing sensitivity. However, the MB shows a different behavior; it decreases in the negative regime and then increases in the positive regime with increasing AMF for $\text{AMF} < 1.6$, and then gradually decreases with increasing AMF. For the high AOD case, however, a high AMF does not seem to guarantee retrieval stability; the standard deviation is uncorrelated with AMF. For the test-bed algorithm, the MB tends to decrease with increasing AMF except for the bifurcation observed for $\text{AMF} < 1.5$, while no dependency is observable for the C005 algorithm.

5 Conclusions

We quantitatively assessed the effects of new aerosol models on AOD retrieval from spectral reflectance observed by Aqua-MODIS over the global ocean for the period from 2003 to 2010. AERONET inversion data and the optical property data of tri-axial ellipsoidal dust particles from an existing database were used to archive AOP to calculate LUTs, accounting for various aerosol types from absorbing to non-absorbing ($0.85 < \text{SSA} < 1.00$) and from fine particle- to coarse particle-dominated

Aerosol optical depth retrieval from MODIS spectral reflectance

J. Lee et al.

Title Page

Abstract

Introduction

Conclusions

References

Tables

Figures

◀

▶

◀

▶

Back

Close

Full Screen / Esc

Printer-friendly Version

Interactive Discussion



(0.2 or $0.3 < \text{FMF} < 1.0$). Because the C005 algorithm considers only water-soluble aerosols with/without humidity for fine-mode and sea salt/dust for coarse-mode, there was a noticeable difference in AOD retrieval using the new algorithms because of the consideration of absorptivity of fine-mode aerosols and the size distribution shift as a function of AOD.

Validation of the algorithms using eight years of data revealed that the new aerosol models improved the AOD, with a regression equation of $y = 0.99x + 0.007$ and a Pearson coefficient of 0.93 compared to $y = 0.85x + 0.028$ and 0.92, respectively, for the C005 algorithm. The percentage of AOD data falling within the expected error was 64 % for the test-bed and 62 % for the current operational data. In particular, improvements were noted in the high AOD regime ($\text{AOD} > 0.3$) where the aerosol signal dominates the surface signal; there was a 12 % increase in the number of reliable data points within the expected error. The root mean squared error (RMSE) and MB also improved when the test-bed algorithm was used.

To further characterize the retrieval errors, the data were validated with respect to AE, scattering angle, and AMF. The new aerosol models mitigated the dependence of MB (systematic error) on the aforementioned parameters. However, the coarse particle-dominated AOD was still overestimated and the fine particle-dominated AOD was underestimated. While the systematic overestimation of the coarse particle-dominated AOD increased for the high AOD case, the results for the fine particle-dominated AOD cases were similar compared to the overall case. Retrieval stability, however, was higher for the coarse particle-dominated case than the fine particle-dominated case, partly due to the wider variability of optical properties of the fine-mode aerosols. The test-bed algorithm significantly reduced the scattering angle dependence of retrieval error for dust-dominated cases ($\text{AE} < 0.8$, $\text{AOD} > 0.3$) partly due to improved treatment of the nonsphericity of dust particles. The standard deviation of the retrieval errors tended to decrease with AMF overall as expected, but no distinct tendency was observed for $\text{AOD} > 0.3$. Our validation results indicate that the aerosol models adopted in the current MODIS operational algorithm need to be updated to achieve better accuracy.

Aerosol optical depth retrieval from MODIS spectral reflectance

J. Lee et al.

[Title Page](#)[Abstract](#)[Introduction](#)[Conclusions](#)[References](#)[Tables](#)[Figures](#)[◀](#)[▶](#)[◀](#)[▶](#)[Back](#)[Close](#)[Full Screen / Esc](#)[Printer-friendly Version](#)[Interactive Discussion](#)

Further analyses with size-resolved AOD are required to obtain a better understanding of the anthropogenic contribution to radiative forcing and air quality.

Acknowledgements. We thank the principal investigators and their staff for establishing and maintaining the AERONET sites used in this investigation. This work was supported by National Institute of Environmental Research (NIER) of Korea (Grant NO. 1600-1637-303-210-13) and was a part of the project titled “Support for research and application of Geostationary Ocean Color Imager (GOCI)” funded by the Ministry of Land, Transport, and Maritime Affairs, Korea. Jhoon Kim and Jaehwa Lee received partial funding for this project from the Brain Korea 21 (BK21) program. Ping Yang acknowledges support from the National Science Foundation (ATM-0803779) of the United States.

References

- Bi, L., Yang, P., Kattawar, G. W., and Kahn, R.: Single-scattering properties of triaxial ellipsoidal particles for a size parameter range from the Rayleigh to geometric-optics regimes, *Appl. Optics*, 48(1), 114–126, 2009.
- Bohren, C. F. and Huffman, D. R.: *Absorption and scattering of light by small particles*, Wiley-Interscience, New York, 1983.
- Chu, D. A., Kaufman, Y. J., Ichoku, C., Remer, L. A., Tanré, D., and Holben, B. N.: Validation of MODIS aerosol optical depth retrieval over land, *Geophys. Res. Lett.*, 29, 8007, doi:10.1029/2001GL013205, 2002.
- Dubovik, O. and King, M. D.: A flexible inversion algorithm for retrieval of aerosol optical properties from sun and sky radiance measurements, *J. Geophys. Res.*, 105, 20673–20696, 2000.
- Dubovik, O., Holben, B. N., Eck, T. F., Smirnov, A., Kaufman, Y. J., King, M. D., Tanré, D., and Slutsker, I.: Variability of absorption and optical properties of key aerosol types observed in worldwide locations, *J. Atmos. Sci.*, 59, 590–608, 2002.
- Dubovik, O., Sinyuk, A., Lapyonok, T., Holben, B. N., Mishchenko, M., Yang, P., Eck, T. F., Volten, H., Muñoz, O., Veihelmann, B., van der Zande, W. J., Leon, J.-F., Sorokin, M., and Slutsker, I.: Application of spheroid models to account for aerosol particle nonsphericity in remote sensing of desert dust, *J. Geophys. Res.*, 111, D11208, doi:10.1029/2005JD006619, 2006.

Aerosol optical depth retrieval from MODIS spectral reflectance

J. Lee et al.

Title Page

Abstract

Introduction

Conclusions

References

Tables

Figures

◀

▶

◀

▶

Back

Close

Full Screen / Esc

Printer-friendly Version

Interactive Discussion



Aerosol optical depth retrieval from MODIS spectral reflectance

J. Lee et al.

Title Page

Abstract

Introduction

Conclusions

References

Tables

Figures

◀

▶

◀

▶

Back

Close

Full Screen / Esc

Printer-friendly Version

Interactive Discussion



- Hess, M., Koepke, P., and Schult, I.: Optical properties of aerosols and clouds: The software package OPAC, *B. Am. Meteorol. Soc.*, 79, 831–844, 1998.
- Higurashi, A. and Nakajima, T.: Development of a two-channel aerosol retrieval algorithm on a global scale using NOAA AVHRR, *J. Atmos. Sci.*, 56, 924–941, 1999.
- 5 Higurashi, A. and Nakajima, T.: Detection of aerosol types over the East China Sea near Japan from four-channel satellite data, *Geophys. Res. Lett.*, 29(17), 1836, doi:10.1029/2002GL015357, 2002.
- Holben, B. N., Eck, T. F., Slutsker, I., Tanré, D., Buis, J. P., Setzer, A., Vermote, E., Reagan, J. A., Kaufman, Y. J., Nakajima, T., Lavenu, F., Jankowiak, I., and Smirnov, A.: AERONET – a federated instrument network and data archive for aerosol characterization, *Remote Sens. Environ.*, 66, 1–16, 1998.
- 10 Hsu, N. C., Tsay, S. C., King, M. D., and Herman, J. R.: Aerosol retrievals over bright-reflecting source regions, *IEEE T. Geosci. Remote*, 42(3), 557–569, 2004.
- Hsu, N. C., Tsay, S. C., King, M. D., and Herman, J. R.: Deep blue retrievals of Asian aerosol properties during ACE-Asia, *IEEE T. Geosci. Remote*, 44(11), 3180–3195, 2006.
- 15 Ichoku, C., Chu, D. A., Mattoo, S., Kaufman, Y. J., Remer, L. A., Tanré, D., Slutsker, I., and Holben, B. N.: A spatio-temporal approach for global validation and analysis of MODIS aerosol products, *Geophys. Res. Lett.*, 29(12), 8006, doi:10.1029/2001GL013206, 2002.
- IPCC, *Climate Change 2007: The Physical Science Basis*, Contribution of Working Group I to the Fourth Assessment Report of the Intergovernmental Panel on Climate Change, edited by: Solomon, S., Qin, D., Manning, M., Chen, Z., Marquis, M., Averyt, K. B., Tignor, M., and Miller, H. L., Cambridge University Press, Cambridge, UK and New York, NY, USA, 2007.
- 20 Jethva, H., Satheesh, S. K., Srinivasan, J., and Levy, R. C.: Improved retrieval of aerosol size-resolved properties from moderate resolution imaging spectroradiometer over India: role of aerosol model and surface reflectance, *J. Geophys. Res.*, 115, D18213, doi:10.1029/2009JD013218, 2010.
- Kaufman, Y. J., Tanré, D., Remer, L. A., Vermote, E. F., Chu, A., and Holben, B. N.: Operational remote sensing of tropospheric aerosol over land from EOS moderate resolution imaging spectroradiometer, *J. Geophys. Res.*, 102(D14), 17051–17067, 1997.
- 30 Kim, J., Lee, J., Lee, H. C., Higurashi, A., Takemura, T., and Song, C. H.: Consistency of the aerosol type classification from satellite remote sensing during the Atmospheric Brown Cloud–East Asia Regional Experiment campaign, *J. Geophys. Res.*, 112, D22S33, doi:10.1029/2006JD008201, 2007.

Aerosol optical depth retrieval from MODIS spectral reflectance

J. Lee et al.

Title Page

Abstract

Introduction

Conclusions

References

Tables

Figures

◀

▶

◀

▶

Back

Close

Full Screen / Esc

Printer-friendly Version

Interactive Discussion



Kim, J., Yoon, J.-M., Ahn, M. H., Sohn, B. J., and Lim, H. S.: Retrieving aerosol optical depth using visible and mid-IR channels from geostationary satellite MTSAT-1R, *Int. J. Remote Sens.*, 29(21), 6181–6192, 2008.

Knapp, K. R., Vonder Haar, T. H., and Kaufman, Y. J.: Aerosol optical depth retrieval from GOES-8: uncertainty study and retrieval validation over South America, *J. Geophys. Res.*, 107, D74055, doi:10.1029/2001JD000505, 2002.

Lee, J., Kim, J., Song, C. H., Kim, S. B., Chun, Y., Sohn, B. J., and Holben, B. N.: Characteristics of aerosol types from AERONET sunphotometer measurements, *Atmos. Environ.*, 44, 3110–3117, doi:10.1016/j.atmosenv.2010.05.035, 2010a.

Lee, J., Kim, J., Song, C. H., Ryu, J.-H., Ahn, Y.-H., and Song, C. K.: Algorithm for retrieval of aerosol optical properties over the ocean from the geostationary ocean color imager, *Remote Sens. Environ.*, 114, 1077–1088, doi:10.1016/j.rse.2009.12.021, 2010b.

Levy, R. C., Remer, L. A., and Dubovik, O.: Global aerosol optical properties and application to Moderate Resolution Imaging Spectroradiometer aerosol retrieval over land, *J. Geophys. Res.*, 112, D13210, doi:10.1029/2006JD007815, 2007a.

Levy, R. C., Remer, L. A., Mattoo, S., Vermote, E. F., and Kaufman, Y. J.: Second-generation operational algorithm: Retrieval of aerosol properties over land from inversion of Moderate Resolution Imaging Spectroradiometer spectral reflectance, *J. Geophys. Res.*, 112, D13211, doi:10.1029/2006JD007811, 2007b.

Levy, R. C., Remer, L. A., Kleidman, R. G., Mattoo, S., Ichoku, C., Kahn, R., and Eck, T. F.: Global evaluation of the Collection 5 MODIS dark-target aerosol products over land, *Atmos. Chem. Phys.*, 10, 10399–10420, doi:10.5194/acp-10-10399-2010, 2010.

Meng, Z., Yang, P., Kattawar, G. W., Bi, L., Liou, K. N., and Laszlo, I.: Single-scattering properties of tri-axial ellipsoidal mineral dust aerosols: a database for application to radiative transfer calculations, *J. Aerosol Sci.*, 41, 501–512, doi:10.1016/j.jaerosci.2010.02.008, 2010.

Mielonen, T., Arola, A., Komppula, M., Kukkonen, J., Koskinen, J., de Leeuw, G., and Lehtinen, K. E. J.: Comparison of CALIOP level 2 aerosol subtypes to aerosol types derived from AERONET inversion data, *Geophys. Res. Lett.*, 36, L18804, doi:10.1029/2009GL039609, 2009.

Mishchenko, M. I. and Travis, L. D.: Capabilities and limitations of a current FORTRAN implementation of the T-matrix method for randomly oriented rotationally symmetric scatterers, *J. Quant. Spectrosc. Ra.*, 60, 309–324, 1998.

Mishchenko, M. I., Geogdzhayev, I. V., Cairns, B., Rossow, W. B., and Lacis, A. A.: Aerosol

Aerosol optical depth retrieval from MODIS spectral reflectance

J. Lee et al.

Title Page

Abstract

Introduction

Conclusions

References

Tables

Figures

◀

▶

◀

▶

Back

Close

Full Screen / Esc

Printer-friendly Version

Interactive Discussion



retrievals over the ocean by use of channels 1 and 2 AVHRR data: Sensitivity analysis and preliminary results, *Appl. Optics*, 38, 7325–7341, 1999.

Pope, C. A. and Dockery, D. W.: Health effects of fine particulate air pollution: Lines that connect, *J. Air Waste Manage.*, 56(6), 709–742, 2006.

5 Remer, L. A., Tanré, D., Kaufman, Y. J., Ichoku, C., Mattoo, S., Levy, R., Chu, D. A., Holben, B., Dubovik, O., Smirnov, A., Martins, J. V., Li, R.-R., and Ahmad, Z.: Validation of MODIS aerosol retrieval over ocean, *Geophys. Res. Lett.*, 29(12), 8008, doi:10.1029/2001GL013204, 2002.

10 Remer, L. A., Kaufman, Y. J., Tanré, D., Mattoo, S., Chu, D. A., Martins, J. V., Li, R.-R., Ichoku, C., Levy, R. C., Kleidman, R. G., Eck, T. F., Vermote, E., and Holben, B. N.: The MODIS aerosol algorithm, products and validation, *J. Atmos. Sci.*, 62, 947–973, 2005.

Remer, L. A., Kleidman, R. G., Levy, R. C., Kaufman, Y. J., Tanré, D., Mattoo, S., Martins, J. V., Ichoku, C., Koren, I., Yu, H., and Holben, B. N.: Global aerosol climatology from the MODIS satellite sensors, *J. Geophys. Res.*, 113, D14S07, doi:10.1029/2007JD009661, 2008.

15 Tanré, D., Kaufman, Y. J., Herman, M., and Mattoo, S.: Remote sensing of aerosol properties over oceans using the MODIS/EOS spectral radiances, *J. Geophys. Res.*, 102(D14), 16971–16988, 1997.

20 Wang, J. and Martin, S. T.: Satellite characterization of urban aerosols: importance of including hygroscopicity and mixing state in the retrieval algorithms, *J. Geophys. Res.*, 112, D17203. doi:10.1029/2006JD008078, 2007.

Wang, J., Christopher, S. A., Brechtel, F., Kim, J., Schmid, B., Redemann, J., Russell, P. B., Quinn, P., and Holben, B. N.: Geostationary satellite retrievals of aerosol optical thickness during ACE-Asia, *J. Geophys. Res.*, 108, 1–14, 2003.

25 Yang, P. and Liou, K. N.: Geometric-optics-integral-equation method for light scattering by non-spherical ice crystals, *Appl. Optics*, 35(33), 6568–6584, 1996.

Yang, P., Feng, Q., Hong, G., Kattawar, G. W., Wiscombe, W. J., Mishchenko, M. I., Dubovik, O., Laszlo, I., and Sokolik, I. N.: Modeling of the scattering and radiative properties of nonspherical dust-like aerosols, *J. Aerosol Sci.*, 38(10), 995–1014, 2007.

30 Yurkin, M. A. and Hoekstra, A. G.: User Manual for the Discrete Dipole Approximation Code ADDA v. 0.79, available at: http://a-dda.googlecode.com/svn/tags/rel_0.79/doc/manual.pdf, 2009.

Aerosol optical depth retrieval from MODIS spectral reflectance

J. Lee et al.

Table 1. Dimensions of the LUT for the MODIS over-ocean algorithm

Variable Name	No. of Entries	Entries
Wavelength (λ)	7	470, 555, 650, 860, 1240, 1630, 2120 nm (band 3, 4, 1, 2, 5, 6, 7, respectively)
SZA (θ_o)	8	0, 10, ..., 70°
SAZA (θ_s)	8	0, 10, ..., 70°
RAA (ϕ)	19	0, 10, ..., 180°
AOD (τ)	9	0.0, 0.1, 0.3, 0.6, 1.0, 1.5, 2.1, 2.8, 3.6
Aerosol Model	23	Classified by FMF and SSA from AERONET inversion data

SZA: solar zenith angle, SAZA: satellite zenith angle, RAA: relative azimuth angle.

Title Page

Abstract

Introduction

Conclusions

References

Tables

Figures

◀

▶

◀

▶

Back

Close

Full Screen / Esc

Printer-friendly Version

Interactive Discussion



Aerosol optical depth retrieval from MODIS spectral reflectance

J. Lee et al.

Table 2a. Statistics for a comparison of AOD retrieved from the MODIS C005 algorithm and AERONET observations from 2003 to 2010 over the global ocean. The numbers in the parentheses are for AOD (AERONET) > 0.3.

MODIS OP	2003	2004	2005	2006	2007	2008	2009	2010	Overall
<i>R</i>	0.91	0.93	0.92	0.87	0.94	0.92	0.92	0.94	0.92
Slope	0.78	0.87	0.82	0.77	0.9	0.9	0.88	0.87	0.85
<i>y</i> -intercept	0.04	0.02	0.03	0.04	0.02	0.03	0.03	0.03	0.03
Percentage within EE	66 % (38 %)	62 % (37 %)	62 % (40 %)	62 % (40 %)	58 % (28 %)	62 % (43 %)	64 % (44 %)	65 % (54 %)	62 % (39 %)
RMSE	0.06 (0.11)	0.07 (0.13)	0.05 (0.09)	0.05 (0.10)	0.06 (0.11)	0.06 (0.10)	0.05 (0.07)	0.05 (0.07)	0.06 (0.11)
MB	0.00 (−0.06)	0.00 (−0.05)	0.00 (−0.06)	0.00 (−0.06)	0.01 (−0.02)	0.01 (−0.01)	0.02 (−0.02)	0.01 (−0.04)	0.01 (−0.04)
<i>N</i>	393 (50)	451 (77)	441 (47)	346 (30)	377 (38)	336 (30)	347 (29)	264 (24)	2955 (325)

[Title Page](#)
[Abstract](#)
[Introduction](#)
[Conclusions](#)
[References](#)
[Tables](#)
[Figures](#)
[Back](#)
[Close](#)
[Full Screen / Esc](#)
[Printer-friendly Version](#)
[Interactive Discussion](#)


Aerosol optical depth retrieval from MODIS spectral reflectance

J. Lee et al.

Table 2b. Same as in Table 2a except that the test-bed algorithm was used.

This study	2003	2004	2005	2006	2007	2008	2009	2010	Overall
<i>R</i>	0.94	0.96	0.93	0.88	0.94	0.92	0.93	0.94	0.93
Slope	1.01	1.00	0.97	0.91	1.01	1.00	1.01	1.00	0.99
<i>y</i> -intercept	0.01	0.01	0.01	0.02	0.01	0.01	0.01	0.00	0.01
Percentage within EE	64 % (50 %)	65 % (55 %)	65 % (48 %)	62 % (43 %)	59 % (36 %)	61 % (36 %)	66 % (60 %)	67 % (70 %)	64 % (51 %)
RMSE	0.05 (0.08)	0.05 (0.08)	0.05 (0.08)	0.06 (0.10)	0.06 (0.12)	0.06 (0.10)	0.05 (0.09)	0.05 (0.07)	0.05 (0.09)
MB	0.01 (0.02)	0.01 (0.01)	0.00 (0.00)	0.00 (−0.01)	0.01 (0.05)	0.01 (0.04)	0.01 (0.02)	0.00 (0.01)	0.01 (0.02)
<i>N</i>	393 (50)	451 (77)	441 (47)	346 (30)	377 (38)	336 (30)	347 (29)	264 (24)	2955 (325)

[Title Page](#)
[Abstract](#)
[Introduction](#)
[Conclusions](#)
[References](#)
[Tables](#)
[Figures](#)
[⏪](#)
[⏩](#)
[◀](#)
[▶](#)
[Back](#)
[Close](#)
[Full Screen / Esc](#)
[Printer-friendly Version](#)
[Interactive Discussion](#)


Aerosol optical depth retrieval from MODIS spectral reflectance

J. Lee et al.

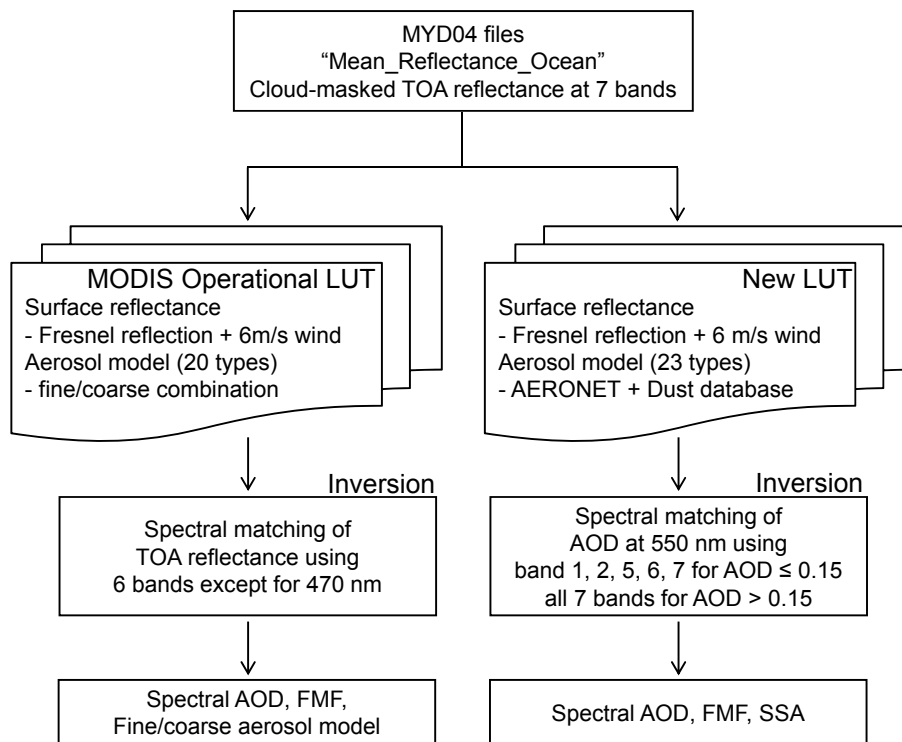


Fig. 1. Schematic flowchart of aerosol retrieval by the MODIS C005 algorithm (left column) and the test-bed algorithm (right column). The test-bed algorithm was designed to use the same observation data (“Mean_Reflectance_Ocean” in “MYD04” files) as the C005 algorithm to evaluate the effects of the new aerosol models only. The major difference between the two algorithms is the aerosol models used to calculate the LUT.

Title Page

Abstract

Introduction

Conclusions

References

Tables

Figures

◀

▶

◀

▶

Back

Close

Full Screen / Esc

Printer-friendly Version

Interactive Discussion



Aerosol optical depth retrieval from MODIS spectral reflectance

J. Lee et al.

Title Page

Abstract

Introduction

Conclusions

References

Tables

Figures

◀

▶

◀

▶

Back

Close

Full Screen / Esc

Printer-friendly Version

Interactive Discussion

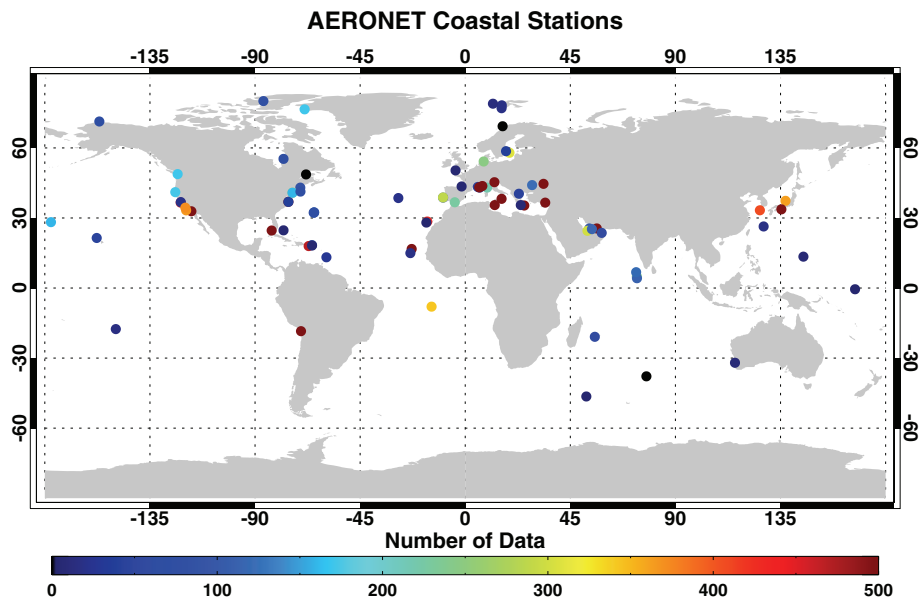


Fig. 2. Global distribution of AERONET sun/sky radiometers located in coastal area (81 stations) used to archive aerosol optical properties for the test-bed algorithm. The colors represent the number of inversion data points at each site. AERONET stations within 7 km from the ocean were chosen as coastal stations.

Aerosol optical depth retrieval from MODIS spectral reflectance

J. Lee et al.

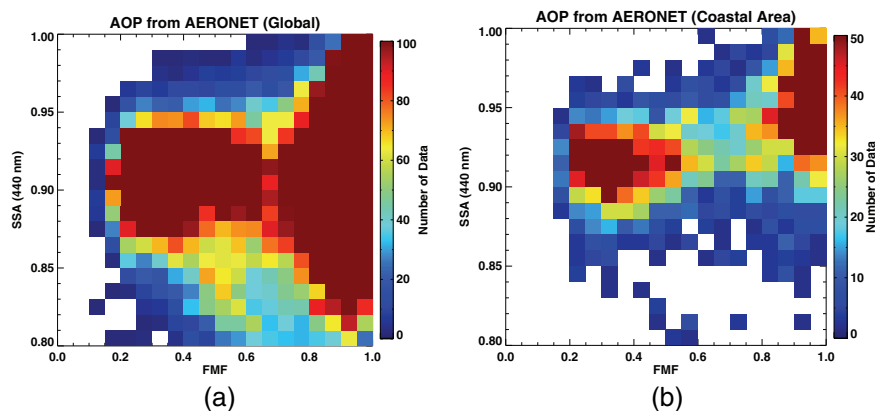


Fig. 3. Number of data points included in each FMF (550 nm) and SSA (440 nm) bin, archived from the AERONET inversion data over **(a)** the globe and **(b)** coastal areas. The data were sorted in intervals of 0.05 and 0.01 for FMF and SSA, respectively. The AERONET stations in the coastal area are shown in Fig. 2.

[Title Page](#)[Abstract](#)[Introduction](#)[Conclusions](#)[References](#)[Tables](#)[Figures](#)[◀](#)[▶](#)[◀](#)[▶](#)[Back](#)[Close](#)[Full Screen / Esc](#)[Printer-friendly Version](#)[Interactive Discussion](#)

Aerosol optical depth retrieval from MODIS spectral reflectance

J. Lee et al.

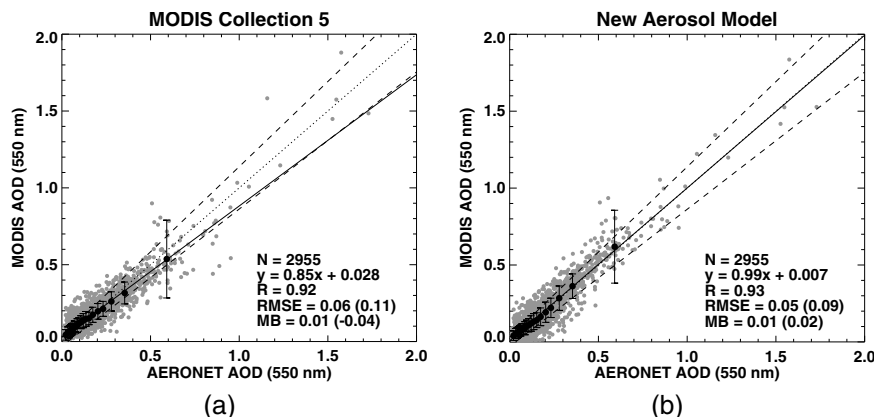


Fig. 4. Comparison of AOD between AERONET and MODIS over the global ocean from 2003 to 2010. The MODIS AODs from (a) the C005 algorithm and (b) the test-bed algorithm with new aerosol models. The collocation criteria of ± 30 min in time and 25 km in space were used. The gray dots represent all data points, whereas black dots with one sigma (standard deviation) interval represent mean AODs in 20 equal-number-of-data bins with respect to the AERONET data. The solid line is from the regression equation, while the dotted and dashed lines are the one-to-one line and the MODIS expected error (EE) line showing $\pm(0.03 + 0.05 \times \text{AOD})$, respectively. Only data points that overlapped between the two algorithms are compared. Originally, the number of data points was 3106 for the C005 algorithm and 3578 for the test-bed algorithm. The statistics shown are the Pearson coefficient (R), root mean squared error (RMSE), mean bias (MB), and the number of data points (N).

Title Page

Abstract

Introduction

Conclusions

References

Tables

Figures

◀

▶

◀

▶

Back

Close

Full Screen / Esc

Printer-friendly Version

Interactive Discussion



Aerosol optical depth retrieval from MODIS spectral reflectance

J. Lee et al.

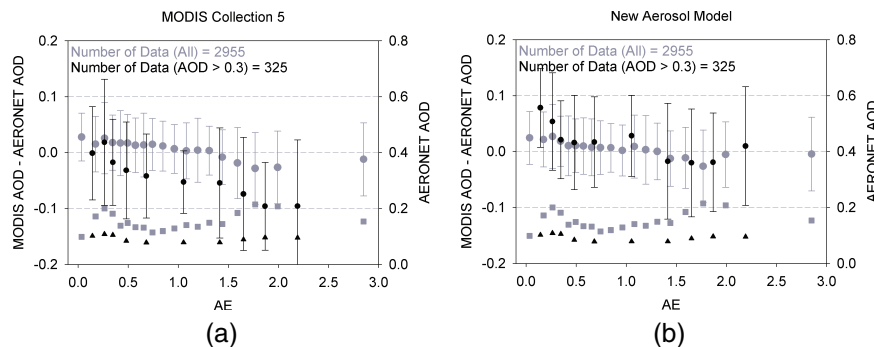


Fig. 5. AE dependence of retrieval errors for **(a)** the C005 algorithm and **(b)** the test-bed algorithm. Gray- and black-colored data points indicate the overall AOD and AOD > 0.3, which were sorted in 20 and 10 equal-number-of-data bins, respectively. The dots and bars represent mean and one sigma intervals of the retrieval errors, respectively, while the gray squares and black triangles ($\times 5$) represent the mean AOD from AERONET in each bin for the overall data and AOD > 0.3, respectively.

Title Page

Abstract

Introduction

Conclusions

References

Tables

Figures

◀

▶

◀

▶

Back

Close

Full Screen / Esc

Printer-friendly Version

Interactive Discussion



Aerosol optical depth retrieval from MODIS spectral reflectance

J. Lee et al.

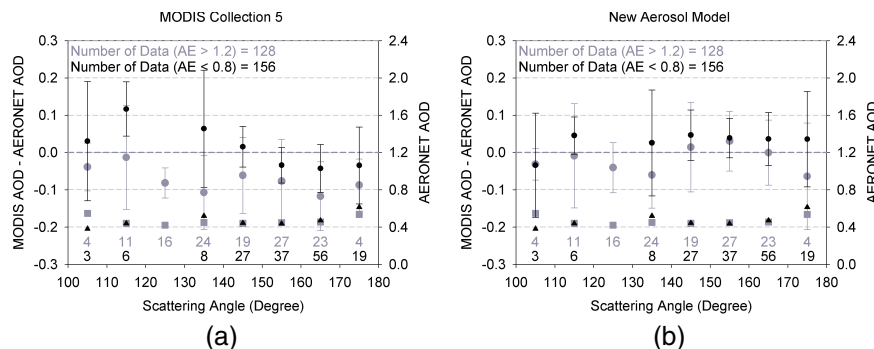


Fig. 6. Scattering angle dependence of the retrieval error. Gray- and black-colored points indicate $AE > 1.2$ and $AE < 0.8$, respectively. Only data with $AOD > 0.3$ were used in this comparison. The symbols and lines are the same as those described in the legend to Fig. 5. Note that the data were sorted in each 10° interval of the scattering angle to highlight differences in the side-scattering-angle range ($100\text{--}130^\circ$) where the number of data points is low. The numbers on the x-axis represent the number of data points in each bin.

Title Page

Abstract

Introduction

Conclusions

References

Tables

Figures

◀

▶

◀

▶

Back

Close

Full Screen / Esc

Printer-friendly Version

Interactive Discussion



Aerosol optical depth retrieval from MODIS spectral reflectance

J. Lee et al.

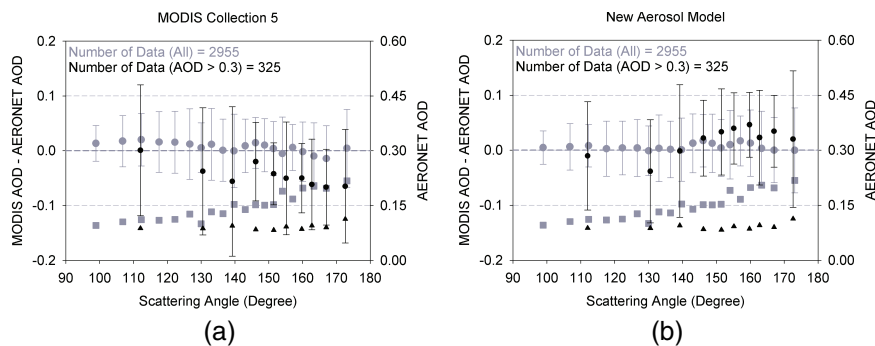


Fig. 7. Scattering angle dependence of retrieval errors for **(a)** the C005 algorithm and **(b)** the test-bed algorithm.

Title Page

Abstract

Introduction

Conclusions

References

Tables

Figures

◀

▶

◀

▶

Back

Close

Full Screen / Esc

Printer-friendly Version

Interactive Discussion



Aerosol optical depth retrieval from MODIS spectral reflectance

J. Lee et al.

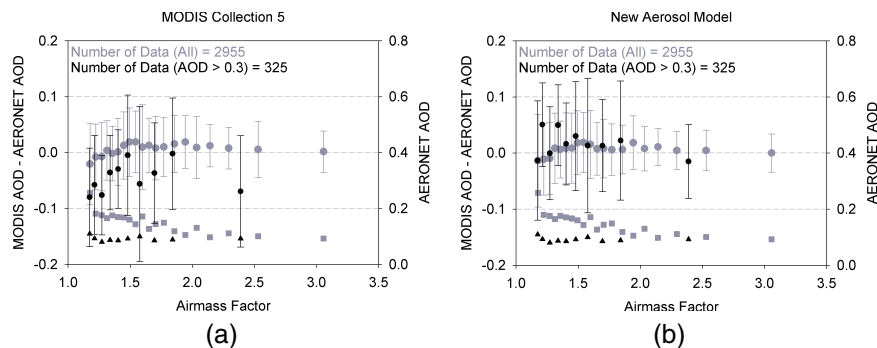


Fig. 8. Air-mass factor ($m_{\text{Sun}} \times m_{\text{satellite}}$, where $m = \sec[\theta]$) dependence of retrieval errors for **(a)** the C05 algorithm and **(b)** the test-bed algorithm.

Title Page

Abstract

Introduction

Conclusions

References

Tables

Figures

◀

▶

◀

▶

Back

Close

Full Screen / Esc

Printer-friendly Version

Interactive Discussion

